물리 계층 네트워크 코딩을 이용한 양방향 중계 채널에서의 정확한 BER 분석

박 문 서*, 최 일 환**, 정회원 안 민 기***, 종신회원 이 인 규****°

Exact BER Analysis of Physical Layer Network Coding for Two-Way Relay Channels

Moonseo Park*, Ilhwan Choi**, Minki Ahn*** *Regular Member*, Inkyu Lee****° *Lifelong Member*

요 약

물리 계층 네트워크 코딩은 양방향 중계 채널에서의 Zhang 그룹의 논문으로 처음 소개 되었다. 물리 계층 네트워크 코딩을 이용하여, 세 개의 시간대 대신에 두 개의 시간대내로 양방향 통신을 완벽히 할 수 있다. 최근 감쇄 채널에서 물리 계층 네트워크 코딩의 상계와 하계가 모두 분석되었다. 이 논문에서는 감쇄 채널에서 양방향 중계 채널의 물리 계층 네트워크 코딩의 정확한 bit 오류 비율을 도출 하였다. bit 오류 비율을 계산하기 위해, 판단 영역을 최소 인접 법칙과 Craig's 극좌표 방식을 적용한 몇 개의 쐐기 부분의 분할을 통해 결정 하였다.

Key Words : Physical Network Coding(PNC), Bit Error Rate(BER), Relay

ABSTRACT

Physical layer network coding (PNC) was first introduce by Zhang et al. for two-way relay channels (TWRCs). By utilizing the PNC, we can complete two-way communications within two time slots, instead of three time slots required in non-PNC systems. Recently, the upper and lower bounds for a bit error rate (BER) of PNC have been analyzed for fading channels. In this paper, we derive an exact BER of the PNC for the TWRC over fading channels. We determine decision regions based on the nearest neighbor rule and partition them into several wedge areas to apply the Craig's polar coordinate form for computing the BER. We confirm that our derived analysis accurately matches with the simulation results.

Ⅰ. Introduction

Recently, two-way relay channel (TWRC) where the relay node conveys the communication between two user nodes has drawn much attention. The relay node may adopt an amplify-and-forward (AF) protocol[1] or a decode-and-forward (DF) protocol[2]. The DF scheme can be improved by employing physical layer network coding (PNC)[3] in the relay node, which completes the two-way communications within two phases. In [3], the bit error rate (BER)
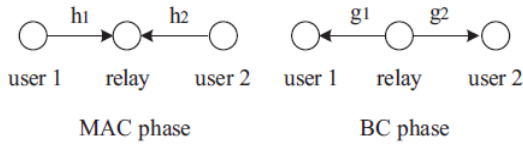
317

Fig. 1. Two-way relay channel model with two phases

of PNC was computed for additive white Gaussian noise (AWGN) channels. In this paper, we analyze the BER of the PNC over fading channels. There are several analysis results on the BER of PNC for non-fading channels[3-5]. In [4], the symbol error rate was derived for AWGN channels where the phase difference between two signals from the two users are either 0 or $\pi/2$. In [5], the BER was computed for the case where the magnitudes of the channels have a Rayleigh fading distribution, but the phase difference between the two channels is assumed to be zero. A symbol error rate analysis for fading channels was done in [6] for non-PNC schemes where bits from the two users are individually detected. Recently, the upper and lower bounds of the BER are derived for the PNC over fading channels in [7]. However, to the best of the authors' knowledge, there is no previous work on the exact BER analysis of the PNC over fading channels. In this paper, we derive an exact BER of the PNC with binary phase shift keying (BPSK) for TWRC over fading channels. To compute the BER, we determine decision regions based on the nearest neighbor rule and divide them into several wedge areas to apply the Craig's polar coordinate form[8]. We confirm that our derived analysis accurately matches with the simulation results.

The rest of this paper is organized as follows: In Section II, we describe the PNC for the TWRC model used in this paper. Section III derives an exact instantaneous BER of PNC for TWRC over fading channels. In Section IV, we provide the numerical results and compare with a non-PNC scheme. Section V concludes the paper.
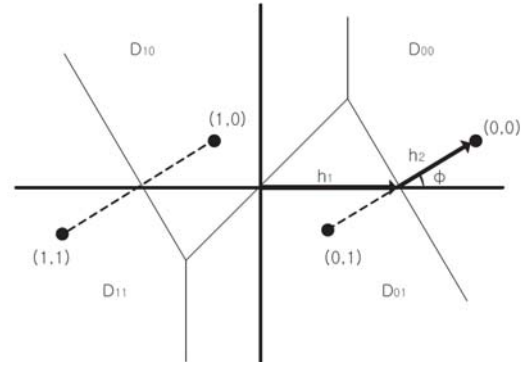
Ⅱ. SYSTEM MODEL

Fig. 2. Decision regions of the received signal at the relay

Fig. 1 shows a communications system using the PNC for the TWRC. The relay and the users are assumed fully symbolsynchronized. We also assume that channel state information is available at the receiver side for both the multiple access channel (MAC) and broadcast channel (BC) phases.

During the MAC phase, the two users, user 1 and user 2, simultaneously transmit the signals x_1 and x_2, respectively, to the relay. We assume that each user employs BPSK signaling. The transmit signal $x_k \in \{1, -1\}$ is generated corresponding to the user k's message $m_k \in \{0, 1\}$. The signals are transmitted over fading channels and the received signal at the relay is given by

$$r = h_1 x_1 + h_2 x_2 + n$$

where h_1 and h_2 represent the channel gains and n indicates the complex Gaussian noise with zero mean and variance σ^2.

Given the received signal r, the relay makes a decision on $m \equiv m_1 \oplus m_2$. The maximum likelihood (ML) detection rule [7] decides $\hat{m} = 0$ if

$$\sum_{m_1 \oplus m_2 = 0} \exp\left[-\frac{|r - h_1 x_1(m_1) - h_2 x_2(m_2)|^2}{2\sigma^2}\right]$$
$$> \sum_{m_1 \oplus m_2 = 1} \exp\left[-\frac{|r - h_1 x_1(m_1) - h_2 x_2(m_2)|^2}{2\sigma^2}\right]$$

and decides $\hat{m} = 1$ otherwise, where $x_k(i)$ represents the signal transmitted by user k when $m_k = i$.

The ML rule described above involves the

computation of exponential functions. In this paper, to simplify the detection, we adopt the nearest neighbor rule [4] [7] [9], which estimates the joint symbols as

$$(\widehat{m_1}, \widehat{m_2}) = \arg\min_{(m_1, m_2)} |r - h_1 x_1(m_1) - h_2 x_2(m_2)|$$

and computes $\widehat{m} \equiv \widehat{m_1} \oplus \widehat{m_2}$. This nearest neighbor rule reduces the detection complexity at the expense of a small performance loss. Fig. 2 exhibits the constellation of the received signal at the relay and the decision regions for the nearest neighbor detection rule. In the figure, (i, j) represents the symbol for the messages $m_1 = i$ and $m_2 = j$, and D_{ij} stands for the decision region for the symbol (i, j).

During the BC phase, the relay broadcasts the BPSK signal $y \in \{1, -1\}$ corresponding to the message $m_r = \widehat{m}$ to both users. The received signal at user k is given by

$$z_k = g_k y + n_k$$

where n_k indicates the complex Gaussian noise with zero mean and variance σ^2.

The users detect the data transmitted by the relay and estimate the message from the other user by applying the XOR operation. For example, user 2 can determine the message from user 1 as

$$\widetilde{m_1} = m_2 \oplus \widetilde{m_{r,2}}$$

where $\widetilde{m_{r,2}}$ represents the estimate of m_r at user 2.

Given channel gains h_i and g_i for $i = 1, 2$, the instantaneous BER at the relay P_{relay} for the MAC phase is written by

$$P_{relay} \equiv \frac{1}{2} [P(\widehat{m} = 1 | m_1 \oplus m_2 = 0) + P(\widehat{m} = 0 | m_1 \oplus m_2 = 1)]$$

Then, the instantaneous end-to-end BER from user 1 to user 2, $P_{1 \to 2}$, is defined as the BER between the data transmitted by user 1 and the data decoded at user 2 given by

$$\begin{aligned} P_{1 \to 2} &\equiv P(\widetilde{m_1} \neq m_1) \\ &= 1 - (1 - P_{relay})(1 - P_{r,2}) - P_{relay} P_{r,2} \\ &= P_{relay} + P_{r,2} - 2 P_{relay} P_{r,2} \end{aligned}$$

where $P_{r,2} = Q\left(\sqrt{\frac{|g_2|^2}{\sigma^2}}\right)$ indicates the instantaneous BER during the BC phase from the relay to user 2. Here, the function $Q(x)$ is defined as $Q(x) = \frac{1}{\sqrt{2\pi}} \int_x^\infty e^{-t^2/2} dt$. Also, the instantaneous end-to-end BER from user 2 to user 1, $P_{2 \to 1}$, is expressed in a similar way as

$$\begin{aligned} P_{2 \to 1} &\equiv P(\widetilde{m_2} \neq m_2) \\ &= P_{relay} + P_{r,1} - 2 P_{relay} P_{r,1} \end{aligned}$$

with $P_{r,1} = Q\left(\sqrt{\frac{|g_1|^2}{\sigma^2}}\right)$

Finally, the overall instantaneous end-to-end BER for given channel gains is obtained by

$$P_{inst} = \frac{1}{2}(P_{1 \to 2} + P_{2 \to 1}). \tag{1}$$

In the next section, we derive the exact instantaneous BER at the relay, P_{relay}, for given channels.

Ⅲ. ERROR PROBABILITY ANALYSIS

We first compute the instantaneous BER at the relay for the case of $|h_1| \geq |h_2|$ and $0 \leq \phi \leq \pi/2$, where $\phi \equiv \arg(h_2) - \arg(h_1)$ denotes the phase difference between the two channels. Then we will generalize the derivation for arbitrary channel gains and phase differences.

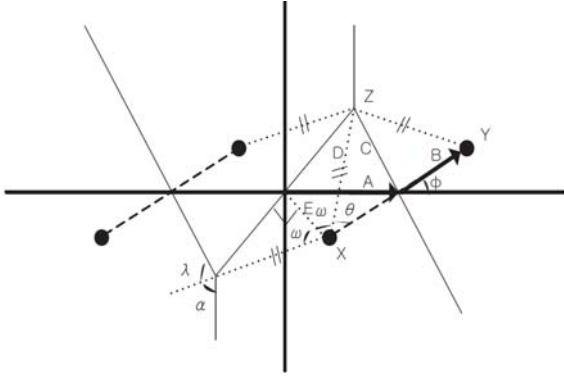A. Derivation of instantaneous BER for $0 < \phi \leq \pi/2$

Fig. 3. Parameters for P_X and P_Y

In this subsection, we derive the exact instantaneous BER at the relay for given channels h_1 and h_2 for $|h_1| \geq |h_2|$ and $0 < \phi \leq \pi/2$. When $\phi = 0$, the decision boundaries become two parallel lines. Thus, the case of $\phi = 0$ will be considered separately in the next subsection. Now the instantaneous BER at the relay P_{relay} is written as

$$P_{relay} \equiv \frac{1}{4}[P(r \in D_{01} \cup D_{10} | (m_1, m_2) = (0,0))$$
$$+ P(r \in D_{00} \cup D_{11} | (m_1, m_2) = (0,1))$$
$$+ P(r \in D_{00} \cup D_{11} | (m_1, m_2) = (1,0))$$
$$+ P(r \in D_{01} \cup D_{10} | (m_1, m_2) = (1,1))].$$

Due to symmetry, we have

$$P(r \in D_{01} \cup D_{10} | (m_1, m_2) = (0,0))$$
$$= P(r \in D_{01} \cup D_{10} | (m_1, m_2) = (1,1))$$

and

$$P(r \in D_{00} \cup D_{11} | (m_1, m_2) = (0,1))$$
$$= P(r \in D_{00} \cup D_{11} | (m_1, m_2) = (1,0)).$$

Thus, P_{relay} is simplified as

$$P_{relay} \equiv \frac{1}{2}(P_X + P_Y), \qquad (2)$$

where

$$P_X \equiv P(r \in D_{00} \cup D_{11} | (m_1, m_2) = (0,1))$$

and

$$P_Y \equiv P(r \in D_{01} \cup D_{10} | (m_1, m_2) = (0,0)).$$

First, we compute P_X as $P_X = P_{X1} + P_{X2}$, where

$$P_{X1} \equiv P(r \in D_{00} | (m_1, m_2) = (0,1))$$

and

$$P_{X2} \equiv P(r \in D_{11} | (m_1, m_2) = (0,1)).$$
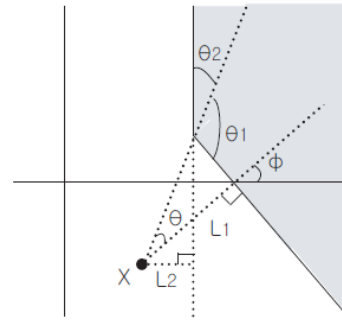
Before proceeding to derive P_{X1}, we define the

Fig. 4. Wedge area for computing P_{X1} for $A < 2B\cos\phi$

following parameters as shown in Fig. 3:

$$A = |h_1|, B = |h_2|, Z_x = B\cos\phi,$$
$$C = (A - Z_x)/\sin\phi = (A - B\cos\phi)/\sin\phi,$$
$$\theta = \arctan\frac{C}{B},$$

where Z_x represents the horizontal component of the point Z. Fig. 3 also presents additional parameters for P_{X2}. These parameters can be calculated as

$$D = B/\cos\theta, X_x = A - B\cos\phi, X_y = -B\sin\phi,$$
$$E = \sqrt{X_x^2 + X_y^2} = \sqrt{A^2 - 2AB\cos\phi + B^2},$$
$$w = \arccos\frac{E}{D}, \alpha = \frac{3}{2}\pi - \phi - \theta - 2w,$$
$$\lambda = \pi - \phi - \alpha = \theta + 2w - \frac{\pi}{2},$$

where X_x and X_y represent the horizontal and the vertical components of the point X, respectively.

Next, we refer to Fig. 4 for deriving P_{X1}, where we divide D_{00} into two wedge areas with angles θ_1 and θ_2. Then we can apply the formula in [8] for each wedge area to obtain

$$P_{X1} = \frac{1}{2\pi}\int_0^{\theta_1} \exp\left[-\frac{L_1^2}{2\sigma^2 \sin^2\varphi}\right]d\varphi$$
$$+ \frac{1}{2\pi}\int_0^{\theta_2} \exp\left[-\frac{L_2^2}{2\sigma^2 \sin^2\varphi}\right]d\varphi.$$

It is easy to show that $\theta_1 = \frac{\pi}{2} + \theta$ and $\theta_2 = \frac{\pi}{2} - \theta - \phi$ from the figure. Also, the distances from the point X to the edge and the extension of one edge of the wedge areas in Fig. 4 are given by $L_1 = B$ and $L_2 = Z_x - X_x = 2B\cos\phi - A$, respectively. Thus, it follows
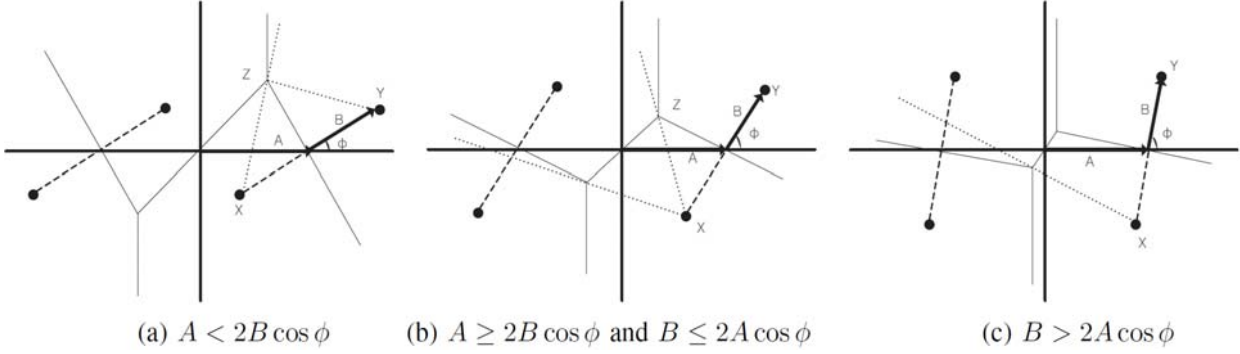
(a) $A < 2B\cos\phi$ (b) $A \geq 2B\cos\phi$ and $B \leq 2A\cos\phi$ (c) $B > 2A\cos\phi$

Fig. 5. Different cases for computing P_X

Fig. 6. Diagram for computing P_{Y1} and P_{Y2}

$$P_{X1} = \frac{1}{2\pi}\int_0^{\frac{\pi}{2}+\theta}\exp\left[-\frac{B^2}{2\sigma^2\sin^2\varphi}\right]d\varphi$$
$$+ \frac{1}{2\pi}\int_0^{\frac{\pi}{2}-\theta-\phi}\exp\left[-\frac{(2B\cos\phi-A)^2}{2\sigma^2\sin^2\varphi}\right]d\varphi.$$

The above derivation of P_{X1} is applied for the case of $Z_x > X_x$, which is equivalent to $A < 2B\cos\phi$. When $Z_x < X_x$, the shape of the diagram changes. Figures 5 (a) and (b) show the

condition for computing P_{X1}. For the case of $A \geq 2B\cos\phi$. in Fig. 5 (b), P_{X1} is obtained in a similar way as

$$P_{X1} = \frac{1}{2\pi}\int_0^{\frac{\pi}{2}+\theta}\exp\left[-\frac{B^2}{2\sigma^2\sin^2\varphi}\right]d\varphi$$
$$- \frac{1}{2\pi}\int_0^{\theta+\phi-\frac{\pi}{2}}\exp\left[-\frac{(A-2B\cos\phi)^2}{2\sigma^2\sin^2\varphi}\right]d\varphi.$$

Now, we address the conditions for computing P_{X2} in figures. 5 (b) and (c). For the case of $B \leq 2A\cos\phi$ in Fig. 5 (b), P_{X2} is given by

$$P_{X2} = \frac{1}{2\pi}\int_0^{\alpha}\exp\left[-\frac{A^2}{2\sigma^2\sin^2\varphi}\right]d\varphi$$
$$+ \frac{1}{2\pi}\int_0^{\lambda}\exp\left[-\frac{(2A\cos\phi-B)^2}{2\sigma^2\sin^2\varphi}\right]d\varphi.$$

Also, for $B > 2A\cos\phi$ in Fig. 5 (c), P_{X2} is written by

$$P_{X2} = \frac{1}{2\pi}\int_0^{\alpha}\exp\left[-\frac{A^2}{2\sigma^2\sin^2\varphi}\right]d\varphi$$
$$- \frac{1}{2\pi}\int_0^{-\lambda}\exp\left[-\frac{(B-2A\cos\phi)^2}{2\sigma^2\sin^2\varphi}\right]d\varphi.$$

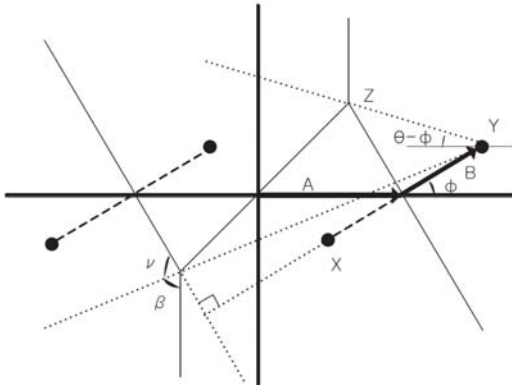Note that λ is nonnegative in (4) and negative in (5).

Next, we consider P_Y which is the probability of bit error given $(m_1, m_2) = (0,0)$. A bit error occurs if the received signal crosses the boundary of the decision region D_{00}. However, if the received signal falls into the decision region D_{11}, the bit error does not occur. Thus, we write

$$P_Y = P_{Y1} - P_{Y2} \text{ where}$$
$$P_{Y1} \equiv P(r \in D_{01} \cup D_{10} \cup D_{11} | (m_1, m_2) = (0,0))$$

and

$$P_{Y2} \equiv P(r \in D_{11} | (m_1, m_2) = (0,0)).$$

Fig. 6 exhibits the diagram for P_{Y1} and P_{Y2}. From this diagram, P_{Y1} is expressed as

$$P_{Y1} = \frac{1}{2\pi}\int_0^{\frac{\pi}{2}-\theta+\phi}\exp\left[-\frac{A^2}{2\sigma^2\sin^2\varphi}\right]d\varphi$$
$$+ \frac{1}{2\pi}\int_0^{\frac{\pi}{2}+\theta}\exp\left[-\frac{B^2}{2\sigma^2\sin^2\varphi}\right]d\varphi.$$

The parameters in Fig. 6 are defined as $\nu = \frac{\pi}{2} - \phi + \arctan\left(\frac{Z_y + B\sin\phi}{A + 2B\cos\phi}\right)$ and $\beta = \pi - \phi - \nu$.

Then P_{Y2} can be obtained as

$$P_{Y2} = \frac{1}{2\pi}\int_0^{\nu}\exp\left[-\frac{(2A\cos\phi+B)^2}{2\sigma^2\sin^2\varphi}\right]d\varphi$$
$$+ \frac{1}{2\pi}\int_0^{\beta}\exp\left[-\frac{(A+2B\cos\phi)^2}{2\sigma^2\sin^2\varphi}\right]d\varphi.$$

B. BER for the channels with $\phi = 0$

In this subsection, we present the instantaneous BER at the relay for $|h_1| \geq |h_2|$ and $\phi = 0$. When
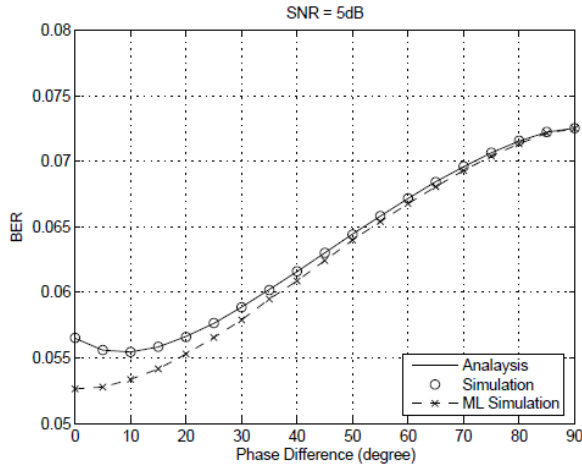
Fig. 7. The instantaneous BERs at the relay of the PNC when $|h_1| = |h_2|$ or various phase differences

the phase difference between the two channels is zero, we can employ the formulae in [4] as

$$P_X = \frac{1}{\pi} \int_0^{\frac{\pi}{2}} \exp\left[-\frac{B^2}{2\sigma^2 \sin^2\varphi}\right] d\varphi + \frac{1}{\pi} \int_0^{\frac{\pi}{2}} \exp\left[-\frac{(2A-B)^2}{2\sigma^2 \sin^2\varphi}\right] d\varphi$$

and

$$P_Y = \frac{1}{\pi} \int_0^{\frac{\pi}{2}} \exp\left[-\frac{B^2}{2\sigma^2 \sin^2\varphi}\right] d\varphi - \frac{1}{\pi} \int_0^{\frac{\pi}{2}} \exp\left[-\frac{(2A+B)^2}{2\sigma^2 \sin^2\varphi}\right] d\varphi.$$

Then applying these results to (2), we can calculate the instantaneous BER.

C. BER for fading channels

Now, we derive the BER for arbitrary fading channels. First, we denote the instantaneous BER in (2) as $P_r(|h_1|, |h_2|, \phi)$ which is valid for the case of $|h_1| \geq |h_2|$ and $0 \leq \phi \leq \frac{\pi}{2}$. Due to symmetry, the instantaneous BER for arbitrary phase differences with $|h_1| \geq |h_2|$ is given by

$$\overline{P_{relay}}(|h_1|, |h_2|, \phi) = \begin{cases} P_r(|h_1|, |h_2|, |\phi|) \\ \qquad if \ 0 \leq |\phi| \leq \frac{\pi}{2} \\ P_r(|h_1|, |h_2|, \pi - |\phi|) \\ \qquad if \ \frac{\pi}{2} < |\phi| \leq \pi. \end{cases}$$

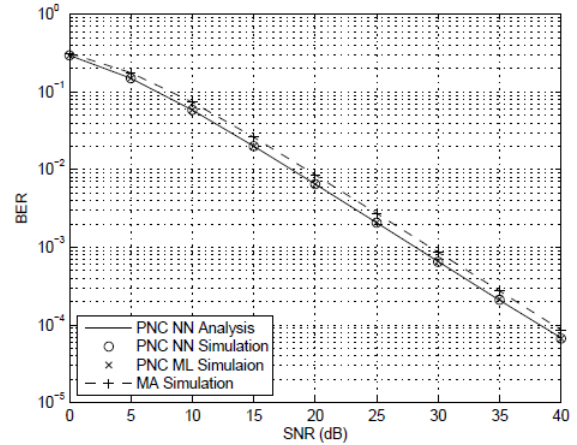Then the instantaneous BER at the relay for

arbitrary channels can be expressed as

$$P_{relay}(|h_1|, |h_2|, \phi) = \begin{cases} \overline{P_{relay}}(|h_1|, |h_2|, \phi) \\ \qquad if \ |h_1| \geq |h_2| \\ \overline{P_{relay}}(|h_1|, |h_2|, \phi) \\ \qquad if \ |h_1| < |h_2|. \end{cases}$$

Once we compute P_{relay}, the instantaneous end-to-end BER P_{inst} can be computed by (1). Finally, the end-to-end BER over fading channels can be obtained by averaging over the fading channel distribution as

$$P_{fading} = \frac{1}{2\pi} \int_0^\infty \int_0^\infty \int_0^{2\pi} P_{inst}(r_1, r_2, \phi) \times f_r(r_1) f_r(r_2) d\phi dr_2 dr_1.$$

Ⅳ. NUMERICAL RESULTS

In this section, we provide numerical results to validate our analysis in Section III. The signal-to-noise ratio (SNR) is defined as the ratio of the average received signal power from one user to the noise power. In our simulation, we implement the nearest neighbor detection scheme for PNC. For comparison, we also evaluate the ML detection scheme and the multiple access (MA) scheme where the bits from user 1 and user 2, m_1 and m_2, are detected individually, instead of detecting only the XORed bit.

Fig. 7 shows the instantaneous BERs at the relay for various values of the phase difference when $|h_1| = |h_2|$ for SNR = 5dB. The optimal result based on ML detection is also plotted. As expected, the

Fig. 8. End-to-end BERs of the PNC and MA schemes over fading channels

BER is smaller as the phase difference decreases. Note that the BER is minimum when the phase difference has a small nonzero value for the nearest neighbor detection.

In the second experiment, the channels are modeled as Rayleigh fadings. The two channels are independently generated using the Monte-Carlo simulation. The BER analysis developed in Section III is used to compute the instantaneous BER for a given channel set, and then the BER is averaged over channel realizations. Fig. 8. presents the BERs of the PNC and the MA schemes. During the BC phase, the relay employs the BPSK modulation for the PNC scheme and 4 QAM for the MA scheme. We assume that the relay consumes the same power as the users and the channels are reciprocal, i.e., $g_k = h_k$. The plot confirms that our analysis results accurately match with the simulation results. The plots also show that the end-to-end BER of the PNC scheme is lower than that of the MA scheme since the BER during the BC phase for the MA scheme is higher than that for the PNC scheme. We can also see that the BER based on the nearest neighbor (NN) detection rule is very close to that based on the ML detection rule.

V. CONCLUSIONS

In this paper, we have analyzed the exact BER of the PNC with BPSK for the TWRC over Rayleigh fading channels. We have confirmed that our analysis results accurately match with the simulation results. The instantaneous BER of the PNC for the TWRC derived in this paper can be applied in many applications. For example, a power control scheme which minimizes the BER can be developed from the result in this paper. As future research directions, the BER performance of the PNC with higher order modulation would be interesting. It would also be useful to find a simpler closed form expression for the BER of the PNC over the fading channels.

References

[1] K.-J. Lee, H. Sung, E. Park, and I. Lee, "Joint Optimization for One and Two-Way MIMO AF Multiple-Relay Systems," IEEE Trans. on Wireless Comms, vol. 9, pp. 3671-3681, Dec. 2010.

[2] R. F.Wyrembelski, T. J. Oechtering and H. Boche, "Decode-and-forward strategies for bidirectional relaying," in Proc. of IEEE-PIMRC, Cannes, France, September 2008.

[3] S. Zhang, S. Liew and P. Lam, "Hot Topic: Physical-Layer Network Coding," in Proc. of ACM MOBICOM '06, Los Angeles, CA, Sep. 2006.

[4] K. Lu, S. Fu, Y. Qian and H.-H. Chen, "SER Performance Analysis for Physical Layer Network Coding over AWGN Channels," in Proc. of IEEE GLOBECOM 2009, Honolulu, HI, Nov. 2009.

[5] E. C. Y. Peh, Y.-C. Liang, and Y. L. Guan, "Power control for physical layer network coding in fading environments," in Proc. of IEEE PIMRC, Cannes, France, Sep. 2008.

[6] A. Y.-C. Peng, S. Yousefi and I.-M. Kim, "On Error Analysis and Distributed Phase Steering for Wireless Network Coding over Fading Channels," IEEE Trans. on Wireless Comm., vol. 8, pp. 5639-5649, Nov. 2009.

[7] M. Ju and I.-M. Kim, "Error Performance Analysis of BPSK Modulation in Physical-Layer Network-Coded Bidirectional Relay Networks," IEEE Trans. on Comm., vol. 58, pp.2770-2775, Oct. 2010.

[8] J. W. Craig, "A New, Simple and Exact Result for Calculating the Probability of Error for Two-Dimensional Signal Constellations," in Proc. IEEE Milcom '91, pp. 571-575, McLean, VA, Nov. 1991.

[9] T. Koike-Akino, P. Popovski and V. Tarokh, "Optimized Constellations for Two-Way Wireless Relaying with Physical Network Coding," IEEE Journal on Selected Areas in Comm., vol. 27, pp. 773-787, June 2009.

박 문 서 (Moonseo Park)

1989년 2월 서울대학교 전기
공학과 졸업
1991년 2월 한국과학기술원
전기 및 전자공학과 석사
1999년 8월 펜실베니아 주립
대 전자공학 박사
2011년 8월~현재 이화여자대
학교 연구 교수
<관심분야> Signal processing and coding theory
for wireless communication, Physical network
coding.
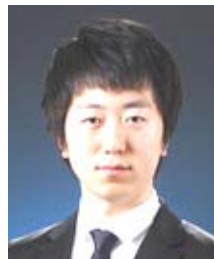
최 일 환 (Ilhwan Choi)

1999년 2월 서강대학교 컴퓨
터공학과 졸업
2001년 2월 서강대학교 컴퓨
터공학과 석사
2001년 2월~현재 삼성전자 재
직중
2011년 8월 고려대학교 전자
전기공학과 박사과정 수료
<관심분야> Signal processing and coding theory
for wireless communication, Multi-user
information theory.

안 민 기 (Minki Ahn)   정회원

2010년 2월 고려대학교 전기
전자전파공학부 졸업
2010년 3월~현재 고려대학교
전자전기공학과 박사과정
<관심분야> multi-user MIMO,
Random Matrix Theory,

이 인 규 (Inkyu Lee)   종신회원

1990년 2월 서울대학교 제어
계측공학과 졸업
1992년 2월 스탠포드대학교
전자공학과 석사
1995년 2월 스탠포드대학교
전자공학과 박사
2002년 9월~현재 고려대학교
전기전자전파공학부 정교수
<관심분야> Digital communications and signal
processing techniques applied for next generation
wireless systems.